

## The influence of the discharge electrode shape on the efficiency of electrostatic precipitator

### Summary

The objective of this experimental study was to investigate the influence of corona electrode design on the collection efficiency. The experiments were carried out with fly ash from lignite combustion in a pulverised-fuel boiler and a fluidized-bed boiler, and with three corona electrodes which differed in design. Current-voltage characteristics and collection efficiency curves were established. The study was performed under laboratory conditions with a horizontal electrostatic precipitator model. The chamber of the experimental setup had a length of 1000 mm, a height of 450 mm and an interelectrode spacing of 400 mm. The results (gathered in tables and plotted in figures) show how the design of the corona electrode and the type of the fly ash affect the collection efficiency under experimental conditions. This finding implies that the optimization of the corona electrode design should include not only the parameters of the electric field, but the physicochemical properties of the fly ash as well.

### 1. Introduction

The new standards for particulate emissions (which have been valid in Poland since January 2004) have imposed the need to retrofit the existing electrostatic precipitators (ESPs) or replace them with new designs capable of providing higher precipitation efficiency. Poland's power plants, as well as thermal-electric power stations, are basically fired with coal, where the proportion of lignite (burnt both in pulverized-fuel and fluidized-bed boiler) is considerable. The performance of the ESP depends on the parameters of the flue gas and fly ash (temperature, humidity, chemical composition, grain size, resistivity), especially when the ESP is coupled with the flue gas desulphurization and denitrification systems, and this has become an increasing tendency nowadays. Despite the great number of investigations – theoretical [1], [2], [3] and experimental [4] – reported in the literature, much effort is still to be made to optimize the geometry of the discharge electrodes and upgrade the collection efficiency of the ESPs for the precipitation of fly ash differing in physicochemical properties [5], [6], [7]. In view of their industrial applications, discharge electrodes should be

- cost effective,
- easy to assemble and disassemble,
- reliable,
- easy to regenerate, and
- capable of providing a high collection efficiency.

The objective of the study reported in this paper was to find an optimal geometry of the discharge electrode for the highest possible precipitation of fly ash which differed in physicochemical properties. Three types of corona electrodes were selected for the purpose of the study. They were tested in a horizontal ESP model under laboratory conditions. The fly ash samples used in the experiments were taken from real flue gases of lignite combustion.

### 2. Theoretical background

Solid particle motion in the ESP can be defined as

$$F_{in} + F_{re} + F_Q = 0 \quad (1)$$

where  $F_{in}$  is force of inertia,  $F_{re}$  stands for the resisting force of dynamic medium, and  $F_Q$  denotes electric force. If we assume that the equation for the resisting force reduces to the Stokes solution, the relation of (1) becomes [8]

$$\frac{dw}{dt} m + 3 \cdot \pi \cdot \eta \cdot d_p \cdot w = Q^\infty E \quad (2)$$

where  $m$  denotes particle mass,  $\eta$  stands for the coefficient of dynamic viscosity,  $d_p$  describes particle diameter,  $w$  is drift velocity,  $Q^\infty$  represents the charge of particle saturation, and  $E$  refers to the electric field strength. Equation (2) can be used to define a drift velocity of the fly ash particle directed vertically to the plane of the collecting electrodes. The efficiency of precipitation in the ESP was described the Deutsch formula [8] :

$$\eta(d) = 1 - \exp\{-De(d, E, v)\} \quad (3)$$

where  $De(d, E, v)$  is the Deutsch number defined as

$$De = \frac{w(d, E)}{h} \cdot \frac{L}{v} \quad (4)$$

where  $L$  stands for the length of the electric field,  $h$  is distance between the discharge electrode and the collecting electrode, and  $v$  denotes gas flow velocity.

The relation of (4) is valid with the following simplifying assumptions:

- fly ash concentration in the cross-section of the ESP is uniform,
- gas velocity in the cross-section of the ESP is uniformly distributed,
- gas velocity in the ESP chamber is constant,
- re-entrainment of precipitated fly ash, reverse corona discharge and fly ash particle collisions are absent.

The application of (4) under industrial conditions promotes errors because the assumptions mentioned above are not fulfilled.

### 3. Experimental

#### 3.1. Laboratory setup

The setup consisted of the following major elements: model of a single-stage ESP chamber, air supply and discharge units, dust particle feeder, high voltage supply and exhaust fan. The ESP chamber was made of Plexiglass to enable visualization of the phenomena that occurred in the interelectrode space. Flat steel plates acted as collecting electrodes. The characteristic parameters of the ESP chamber were as follows: length,  $L$ , 1000mm; height,  $H$ , 450 mm; spacing between collecting and discharge electrode,  $2h=400$  mm; spacing between discharge electrodes,  $s$ , 170 mm. The schematic of the setup is shown in Fig. 1.

The fly ash used in the experiments came from the combustion of lignite in a pulverized-fuel boiler (fly ash K) and a fluidized-bed boiler (fly ash T). The lignite burnt was excavated in the open pits of Konin and Turów, respectively. Figure 2 depicts the particle grain size distribution in the fly ash samples, determined by the sieve method, the grain diameters below 63  $\mu\text{m}$  being established via the centrifugal process (Bahco centrifuge).

The results of physicochemical analyses are summarized in Table 1. Figure 3 shows a photograph of the micrograms of the fly ash particles, obtained with an electron scanning microscope (JEOL, ISM-5800LV)

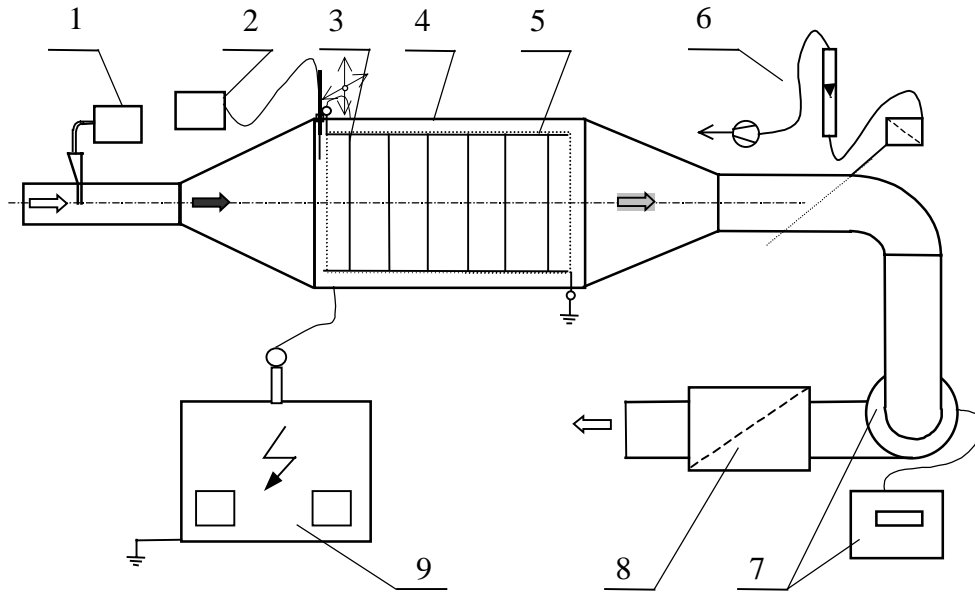


Fig. 1. Experimental setup for testing the discharge electrodes of the ESP model:  
 1 – dust particle feeder, 2 – hot-wire anemometer, 3 – discharge electrodes, 4 – ESP chamber,  
 5 – collecting electrodes, 6 – gravimetric dustmeter, 7 – exhaust fan, 8 – end filter, 9 – high voltage supply.

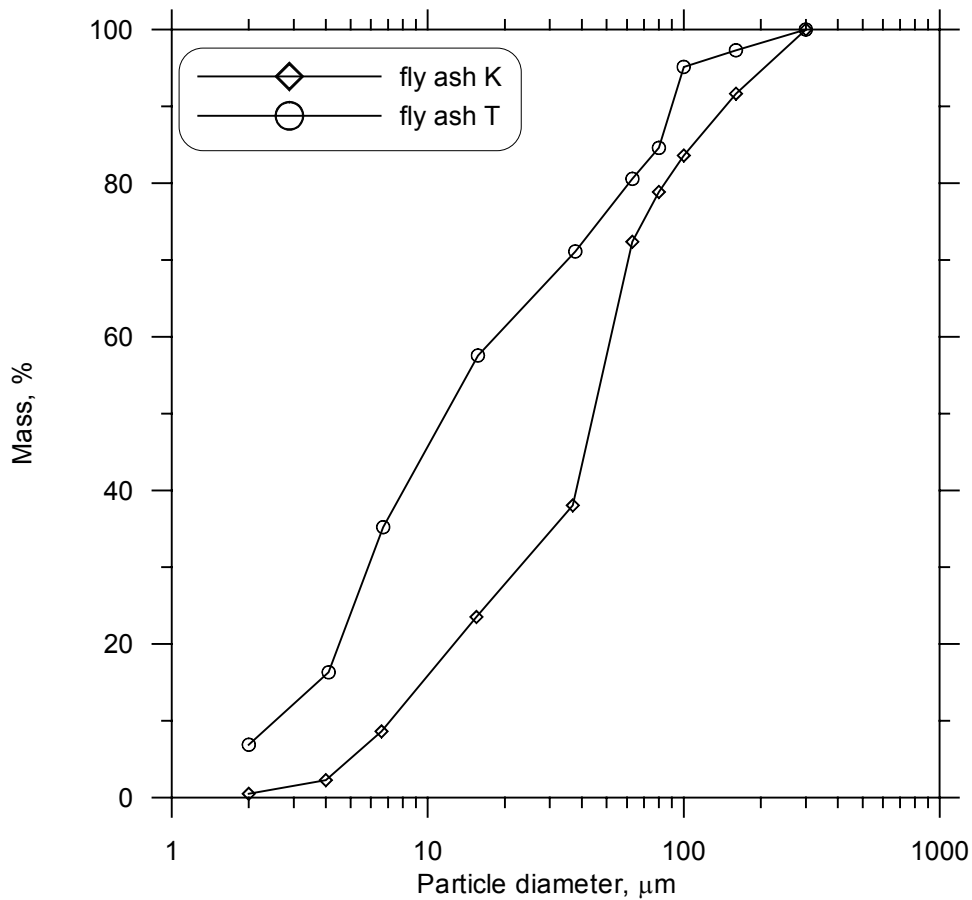
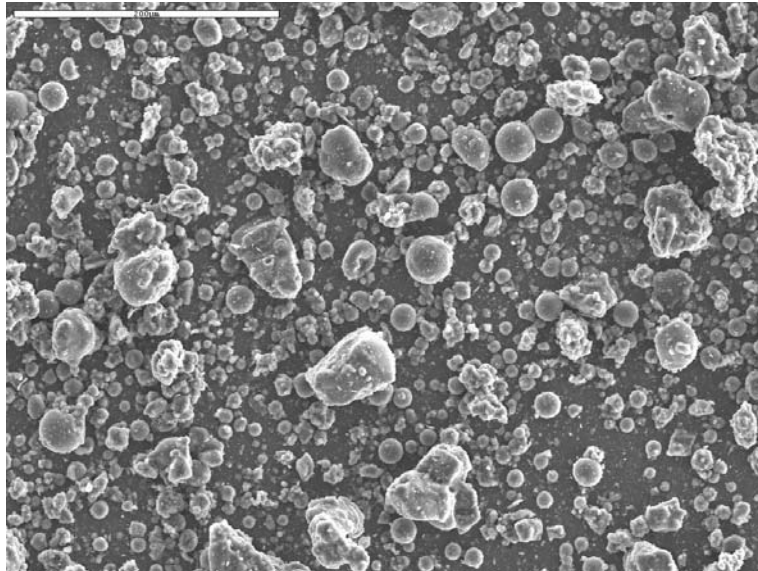


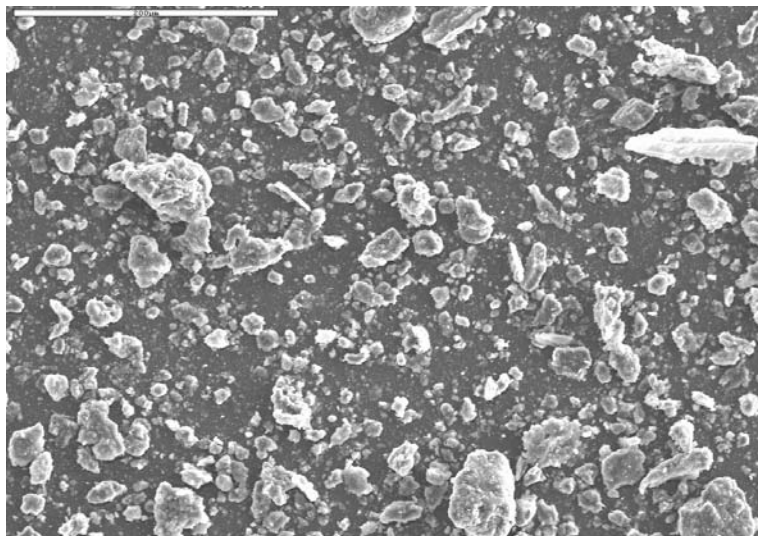
Fig. 2. Particle size distribution of the fly ash tested.

Table 1. Chemical, physical and electrical properties of the fly ash tested

Classification	Value	
Chemical composition	Fly ash K	Fly ash T
	SiO <sub>2</sub> (54.0%)	SiO <sub>2</sub> (36.8%)
	Fe <sub>2</sub> O <sub>3</sub> (4.21%)	Fe <sub>2</sub> O <sub>3</sub> (3.95%)
	Al <sub>2</sub> O <sub>3</sub> (4.42%)	Al <sub>2</sub> O <sub>3</sub> (24.7%)
	Mn <sub>3</sub> O <sub>4</sub> (0.27%)	Mn <sub>3</sub> O <sub>4</sub> (0.04%)
	TiO <sub>2</sub> (1.03%)	TiO <sub>2</sub> (1.75%)
	CaO (25.90%)	CaO (18.10%)
	MgO (4.43%)	MgO (2.19%)
	SO <sub>3</sub> (4.72%)	SO <sub>3</sub> (6.29%)
	P <sub>2</sub> O <sub>5</sub> (0.26%)	P <sub>2</sub> O <sub>5</sub> (0.15%)
	Na <sub>2</sub> O (0.09%)	Na <sub>2</sub> O (1.89%)
	K <sub>2</sub> O (0.24%)	K <sub>2</sub> O (1.08%)
	Unburned carbon in ash	C (0.63%)
Density	2500 (kg/m <sup>3</sup> )	2260 (kg/m <sup>3</sup> )
Resistivity	4.4 x 10 <sup>8</sup> (ohm cm)	5.8 x 10 <sup>8</sup> (ohm cm)



(a)



(b)

Fig. 3. Micrograms of the fly ash particles examined: (a) fly ash from lignite combustion in the pulverized-fuel boiler (fly ash K) (magnification 230x), (b) fly ash from lignite combustion in the fluidized-bed boiler (fly ash T) (magnification 230x).

### 3.2. Methods

Total collection efficiency was established by measurements of fly ash mass at the inlet to, and the outlet from, the ESP. Relevant calculations were carried out using the expression:

$$\eta_{tot} = 1 - \frac{m_{out}}{m_{in}} \cdot 100, \quad \%$$

where  $m_{in}$  and  $m_{out}$  denotes fly ash mass at the inlet and outlet, respectively.

To determine the  $m_{out}$  value, use was made of a gravimetric dustmeter. For aerosol, an isokinetic sampling tube was used to measure the concentration. The dust particles were filtered using high-efficiency filter paper.

Collection efficiency measurements were performed under laboratory conditions, with three types of discharge electrodes differing in design (Fig. 4), at an air temperature of 293 K, a relative air humidity ( $\varphi$ ) of 70%, and gas flow velocities of 0.8 m/s and 1.0 m/s. Gas flow velocity was measured with a constant-temperature hot-wire anemometer of CTA-31 type (Sensor-Electronics, Gliwice, Poland). The discharge electrodes were fed with smoothed constant voltage of negative polarity via a high-voltage power supply (Sørensen HV Supply 1121, 0-100 kV).

### 4. Results

At the initial stage of the study, the current-voltage characteristics for the discharge electrodes (Fig. 4) were determined under clean air conditions. During the experiments the spikes of the electrodes were directed vertically to the plane of the collecting electrode. The results are plotted in Fig. 5. The current-voltage characteristic obtained with dust-laden air samples ( $S = 390 \text{ mg/m}^3$ ) are shown in Fig. 6.

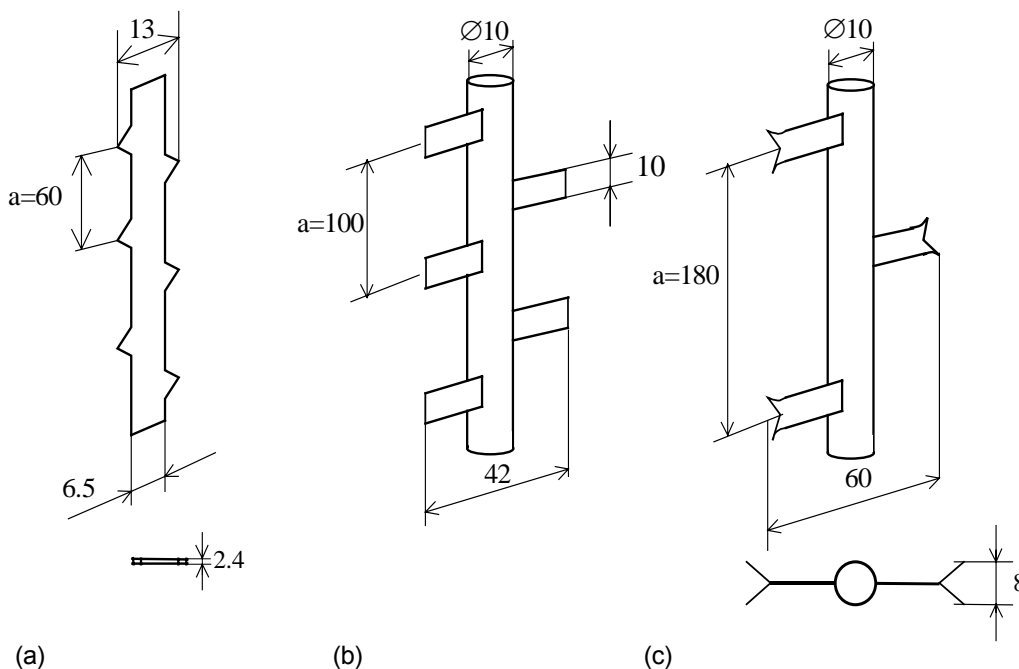


Fig. 4. Design of the discharge electrodes tested: (a) spiked band electrode  $a=60$  mm, (b) pipe and double-spike electrode,  $a=100$  mm (RDE 1), (c) pipe and double-spike electrode,  $a=180$  mm (RDE 2),

With the spiked band electrodes, the corona onset voltage approached 22 kV, compared to that of approximately 15 kV with the pipe and spike electrodes (RDE 1 and RDE 2). The highest and the lowest values of the corona current over the entire supply voltage range were generated by the RDE 1 electrode and the spiked band electrode, respectively. The V-I characteristics of the RDE 2 electrode is flatter than that of the RDE 1, and flat curves yield a lower corona current for the given supply voltage.

Comparing the V-I characteristics obtained under clean air conditions with those determined with dust-laden air samples, we observed in very instance that the corona current measured on the surface of the collecting electrodes was higher when solid particles were present in the interelectrode space (Fig. 6). This is probably due to the fact that a greater number of charge carriers occur in the form of dust particles, though their concentration does not promote the phenomenon of corona suppression.

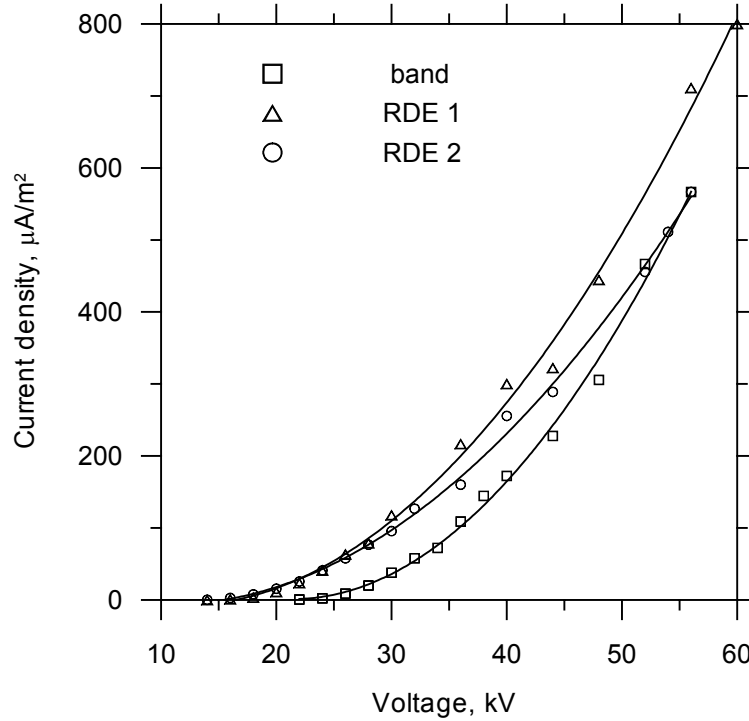


Fig. 5. Current-voltage curves of discharge electrodes tested under air conditions

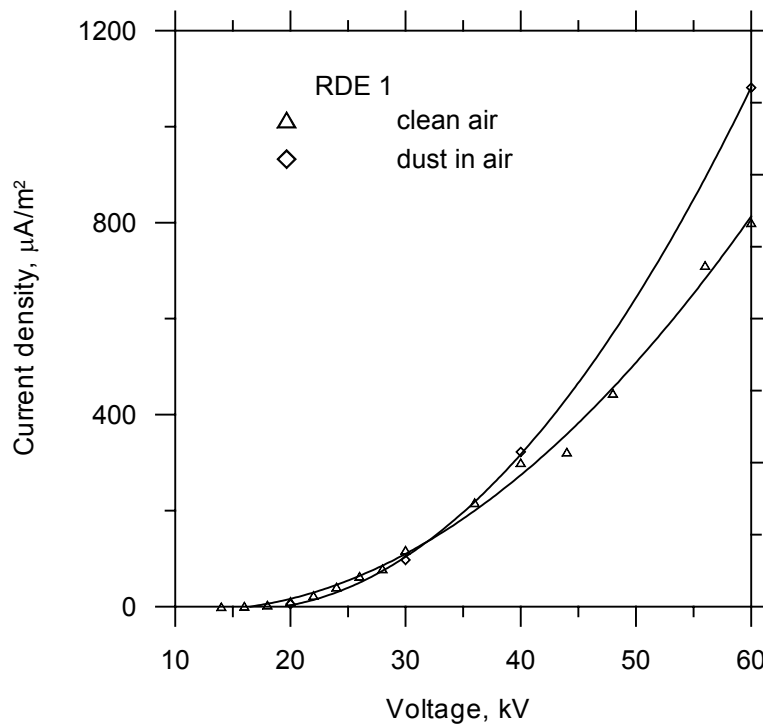


Fig. 6. Current-voltage curves of RDE 1 tested under clean air and dust-laden air conditions

To assess the three electrode designs of choice the collection efficiencies were measured with the ESP model. Efficiency variations for fly ash K are plotted in Figs. 7 and 8, and those for fly ash T in Figs. 9 and 10. As shown by these plots, the collection efficiencies obtained with the gas flow velocity of 0.8 m/s are in every instance higher.

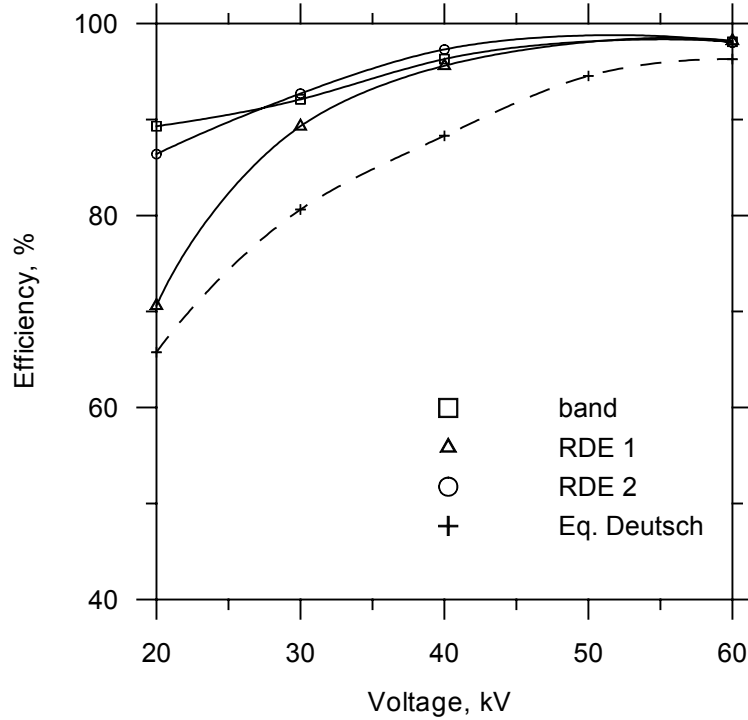


Fig. 7. Collection efficiency of the ESP related to supply voltage for fly ash K ( $v=0.8$  m/s).

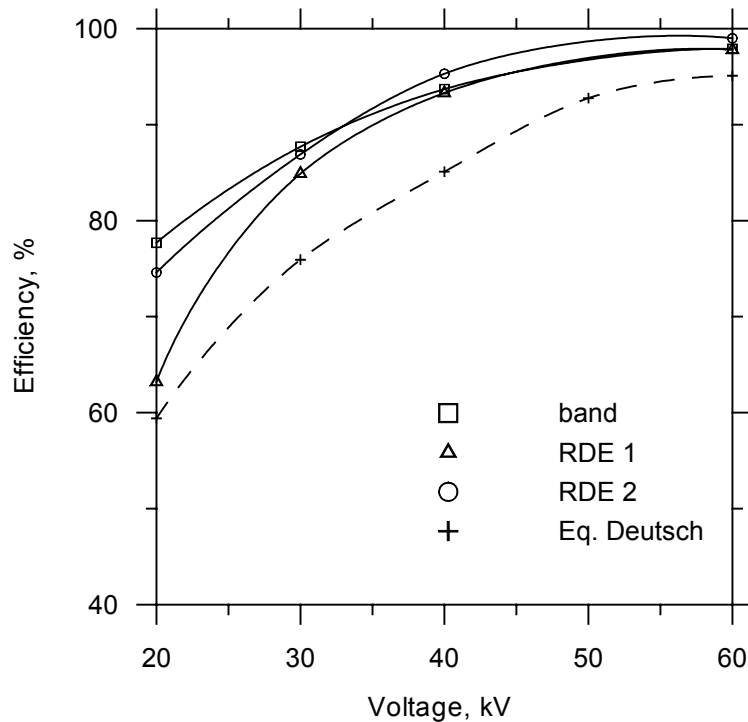


Fig. 8. Collection efficiency of the ESP related to supply voltage for fly ash K ( $v=1.0$  m/s).

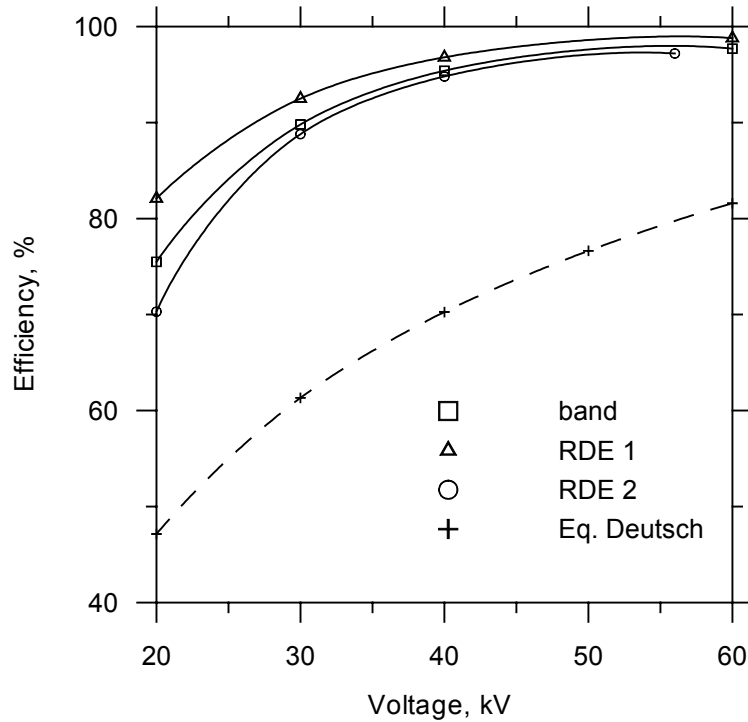


Fig. 9. Collection efficiency of the ESP related to supply voltage for fly ash T ( $v=0.8$  m/s).

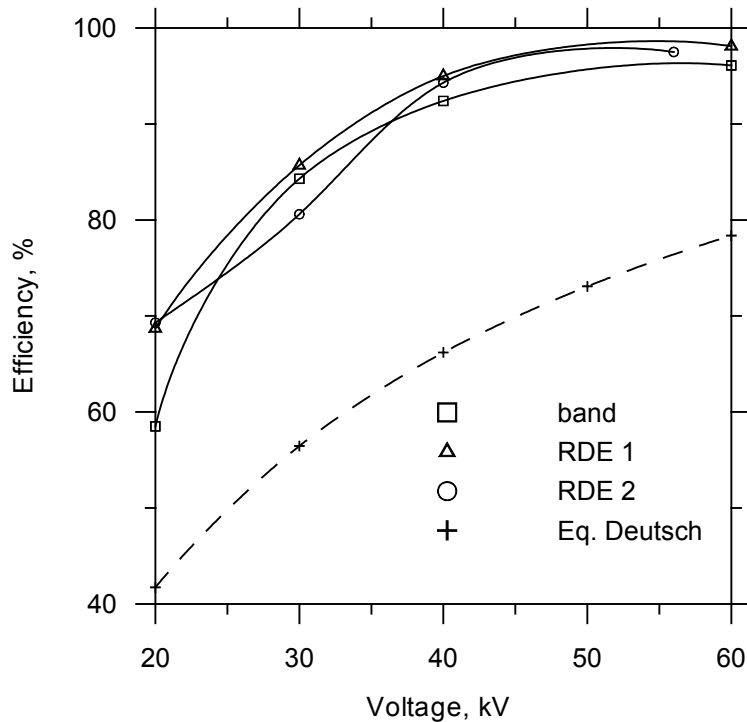


Fig. 10. Collection efficiency of the ESP related to supply voltage for fly ash T ( $v=1.0$  m/s).

A careful examination of the results obtained with the ESP model shows that the precipitation efficiency of the experimental electrodes depends on the physicochemical parameters of the fly ash. As it can be inferred from the analysis of the physicochemical properties of fly ash K and fly ash T, their resistivity is comparable under laboratory conditions. Fly ash K is classified as belonging to the fly ash group of low sodium, potassium and aluminium oxide content. Both fly ash K and fly ash T contain comparatively large amounts of calcium oxide. The proportion of grain size smaller than  $10\ \mu\text{m}$  is greater in fly ash T than in fly ash K, amounting to 46% and 15%, respectively.

With the application of electrode RDE 1 it was possible to achieve a very high precipitation efficiency with respect to fly ash T alone (Figs. 9 and 10). Fly ash K was more efficiently precipitated

with electrode RDE 2 and the spiked band electrode (Figs. 7 and 8). Both the designs have a lower corona current level for the given supply voltage. Comparative analysis has revealed a considerable discrepancy between the experimental and calculated (in terms of the Deutsch formula) collection efficiencies, especially with respect to fly ash T which originated during lignite combustion in a fluidized-bed boiler.

## 5. Summary

The results obtained with the ESP model under laboratory conditions allowed the following generalizations to be made:

- As for fly ash K and fly ash T from lignite combustion in a pulverized-fuel boiler and a fluidized-bed boiler, respectively), it is possible to substitute conventional spiked band electrodes with electrodes of a rigid structure, i.e. with pipe and double-spike electrodes (RDE 1 and RDE 2). Both the designs display a better mechanical strength and operating reliability than spiked band electrodes.
- With these designs of the discharge electrodes, we observed that their collecting efficiency was influenced by the composition of the fly ash.
- Electrode RDE 2 (with a planar current-voltage characteristic) was found to be better suited for the precipitation of fly ash K.
- The RDE 1 electrode (having a current-voltage characteristic of a more 'aggressive' nature than that of the RDE 2 electrode) was more efficient when fly ash T was precipitated.
- The optimization of the corona electrode design should include not only the parameters of the electric field, but also the physicochemical properties of the fly ash. In sum, the choice of an appropriate design for the discharge electrode should be based on a thorough examination of the dust particle-flue gas environment.

## 6. References

- [1] W. Deutsch, Bewegung und Ladung der Elektrizitaetstraeger im Zylinderkondensator. Ann. Physik, Bd. 68, 1922, S.335-344.
- [2] S.H. Kim, K.W. Lee, Experimental study of electrostatic precipitation performance and comparison with existing theoretical prediction models, Journal of Electrostatics 48 (1999), s. 3-25.
- [3] C. Brocilo, J.S. Chang, R.D. Findlay, Modelling of electrode geometry effects on dust collection efficiency of wire-plate electrostatic precipitators, Proceedings: 8th International Conference on Electrostatic Precipitation, May 14-17, 2001, Vol. I, A4-3 Series
- [4] J.D. McCaine, Estimated operating V-I curves for rigid frame discharge electrodes for use in ESP modeling, Proceedings: 8th International Conference on Electrostatic Precipitation, May 14-17, 2001, Vol. I, A4-6 Series.
- [5] M. Jędrusik, J.B. Gajewski, A. Świerczok, Effect of the particle diameter and corona electrode geometry on the particle migration velocity in electrostatic precipitators, Journal of Electrostatics, Vol. 51-52 (2001), p. 245-251.
- [6] J. Miller, B. Hoferer, A.J. Schwab, The impact of corona electrode configuration on electrostatic precipitator performance, Proceedings of the 3<sup>rd</sup> International Conference on Applied Electrostatics, 1997, Shanghai, p.129-137.
- [7] M. Jędrusik, A. Świerczok, R. Teisseyre: Experimental study of fly ash precipitation in a model electrostatic precipitator with discharge electrodes of different design, Powder Technology, 135-136 (2003), p. 295-301.
- [8] K.R. Parker et al.: Applied Electrostatic Precipitation. London, Blackie Academic & Professional, 1997.